

# Non-Hermitian Diffusive Quasicrystal

Zhoufei Liu<sup>1</sup> and Jiping Huang<sup>1,\*</sup>

<sup>1</sup>*Department of Physics, State Key Laboratory of Surface Physics,  
and Key Laboratory of Micro and Nano Photonic Structures (MOE),  
Fudan University, Shanghai 200438, China*

(Dated: August 16, 2022)

## Abstract

Compared with periodic systems, quasicrystals without translational invariance contain more unexpected localization and topological properties. However, most available studies are discussed in the context of quantum systems and classical wave systems. It is still challenging to uncover quasicrystals in diffusion system because of its natural dissipation. Here we construct the one-dimensional Anbry-André-Harper (AAH) model based on the coupled ring chain structure to reveal diffusive quasicrystal. Unlike modulating the onsite potential in wave systems, the incommensurate lattice can be realized in thermal diffusion by only adjusting the parameters. The extended-localized phase transition is demonstrated in the diffusive AAH model. We further present the non-reciprocal AAH model and anti-parity-time symmetric AAH model to discuss the interplay between Anderson localization and non-Hermitian physics. For Anderson localized state, a unique double localization centers phenomenon is shown in the temperature field simulation for all three models. We propose a novel application for double localization centers, which is named as non-Hermitian integrated double-trace distributed generator. Our results can help design flexible thermal devices and achieve efficient heat management.

*Introduction.* The quasicrystal is an ordered but not periodic phase that has received much attention theoretically and experimentally over the last several decades. The most paradigmatic example of a one-dimensional quasicrystal is Aubry-André-Harper (AAH) model [1, 2]. The most unusual feature of the AAH model is that it undergoes a metal-insulator transition at a finite critical value with incommensurate onsite potential due to self-duality [3, 4]. Experimentally, the AAH model has been realized in the quantum systems [5, 6] and classical wave systems [7, 8]. Recently, great interest has been devoted to studying the extended-localized transition [9–12] and topological properties [13–19] of non-Hermitian AAH model, which opens a new door for quasicrystals.

Diffusion system, which is inherently non-Hermitian, plays an important role in heat and mass transfer. Thermal metamaterials [20–22] enable diverse and flexible manipulation of heat flow. Based on transformation thermotics, meaningful progress has been achieved, such as cloaking [23–25] and nonreciprocity [26–28]. Recently, some exotic phases of matter in condensed matter physics have been realized in diffusion systems, such as exceptional point/ring encirclements [29–31], robust edge states [32, 33], one-dimensional Su-Schrieffer-Heeger models [34–37], higher-order topological insulators [38, 39] and non-Hermitian skin effect [40, 41]. However, these works are focused on the periodic systems. The implementation of diffusive quasiperiodic phases has been questioned. Therefore, it is extremely inconvenient but urgently necessary to uncover quasicrystal in diffusion systems.

Here we design coupled ring chain structure to construct the diffusive AAH model. Through modulating the parameters of rings and interlayers, we can derive the diffusive counterpart of the AAH model. Specifically, our diffusive AAH model is a quasiperiodic system that exhibits the extended state and localized state. Next, we study the interplay between non-Hermitian skin effect and Anderson localization. Two skin-Anderson localized transitions can be observed. Finally, the diffusive anti-parity-time (APT) symmetric AAH model is investigated where the extended state is in the APT unbroken phase and the localized state is in the APT broken phase. Interestingly, the temperature fields for Anderson localized state for all models above provide evidence for the presence of two localization centers, which is absent in the quantum systems and classical wave systems. A potential application named as non-Hermitian integrated double-trace distributed generator has been suggested. With its high flexibility, this comprehensive device can generate electricity for two objects simultaneously. Our work may bring new insights into efficient and robust heat manipulation and provide a distinct mechanism of heat insulation.

*Diffusive one-dimensional AAH model.* We start by considering the coupled ring chain structure

as shown in Fig. 1(a). Several rings are vertically coupled in the  $z$  direction to form a chain through interlayers. The interior and exterior radii of rings are denoted by  $R_1$  and  $R_2$ . We can assume  $R_1 \approx R_2 \approx R$  and the perimeter of ring is  $L = 2\pi R$ . The thickness of the ring and interlayer are denoted by  $b$  and  $d$ . Due to Fourier's law in heat conduction, the thermal coupling equation for the  $j$ -th ring can be written as

$$\rho_j C_j \frac{\partial T_j}{\partial t} = \kappa_j \frac{\partial^2 T_j}{\partial x^2} + \rho_j C_j v_j \frac{\partial T_j}{\partial x} + h_{j-1,j}(T_{j-1} - T_j) + h_{j,j}(T_{j+1} - T_j), \quad (1)$$

where  $T_j$ ,  $v_j$ ,  $\kappa_j$ ,  $\rho_j$ , and  $C_j$  are the temperature field, rotating velocity, thermal conductivity, mass density, and heat capacity of the  $j$ -th ring respectively.  $x$  is the position along the ring. The heat exchange rate between the  $(j-1)$ -th interlayer and the  $j$ -th ring is  $h_{j-1,j} = \kappa_{l,j-1}/(\rho_j C_j b d)$ , where  $\kappa_{l,j-1}$  is the thermal conductivity of the  $(j-1)$ -th interlayer. Similarly, the one between the  $j$ -th interlayer and the  $j$ -th ring is  $h_{j,j} = \kappa_{l,j}/(\rho_j C_j b d)$ . As the temperature field of the ring is periodic, we can assume that Eq. (1) has a plane-wave solution with the form  $T_j = A_j e^{i(\beta x - \omega t)}$ . Here  $A_j$  is the amplitude of  $j$ -th ring's temperature field.  $\omega$  is the decay rate.  $\beta = 2m\pi/L = m/R$  is the propagation constant where  $m$  is the mode order. We choose the fundamental mode  $m = 1$  because only the slowest decaying mode can be observed in diffusion systems. Substituting the plane-wave solution into Eq. (1), we can get the effective Hamiltonian of coupled ring chain structure under the open boundary condition, which is written in the second-quantized form:

$$\hat{H} = \sum_j \left[ i h_{j,j+1} \hat{c}_{j+1}^\dagger \hat{c}_j + i h_{j,j} \hat{c}_j^\dagger \hat{c}_{j+1} + (i S_j - \beta v_j) \hat{c}_j^\dagger \hat{c}_j \right], \quad (2)$$

where  $i = \sqrt{-1}$ ,  $\hat{c}_j^\dagger$  and  $\hat{c}_j$  are the creation and annihilation operator of  $j$ -th ring.  $S_j$  is the onsite term with form  $S_j = -(\beta^2 D_j + h_{j-1,j} + h_{j,j})$  in the bulk and  $S_{1(N)} = -(\beta^2 D_{1(N)} + h_{1,1(N-1,N)})$  at the boundary, where  $D_j = \kappa_j/(\rho_j C_j)$  is the diffusivity of the  $j$ -th ring and  $N$  is the number of rings.

Next, we want to map the AAH Hamiltonian onto the ring chain's Hamiltonian. As the AAH model is Hermitian, we can choose the parameters  $\kappa_{l,j} = \kappa_l$  for all interlayers and  $\rho_j = \rho$ ,  $C_j = C$  for all rings. Besides, the velocities of rings are set to zero. So the only parameter that needs to be adjusted here is the ring's thermal conductivity. The effective diffusive AAH Hamiltonian can be written as

$$\hat{H} = \sum_j \left[ i h \hat{c}_{j+1}^\dagger \hat{c}_j + i h \hat{c}_j^\dagger \hat{c}_{j+1} - i (V \cos(2\pi \alpha j) + M h) \hat{c}_j^\dagger \hat{c}_j \right], \quad (3)$$

where  $h = \kappa_l/(\rho C b d)$  is the heat exchange rate,  $\alpha$  is usually an irrational number, and  $V$  is the strength of quasiperiodic potential. Besides, a constant onsite potential must be added to keep

adjusted thermal conductivities positive, where  $M$  is a constant. Detailed derivation of the Hamiltonian and the adjusted thermal conductivities are provided in Part 1 of the Supplemental Material [42]. Here we choose an extended state ( $V = h/2$ ) and a localized state ( $V = 3h$ ) for example. The distributions of adjusted thermal conductivities for both states are shown in Fig. 1(b). Besides, the eigenstate distributions of both states are also shown in Fig. 1(c) and (d). It should be mentioned that here we consider the slowest decaying branch. We perform the simulation of temperature field evolution for both extended state and localized state, as can be seen in Fig. 1(e) and (f). For the extended state, the temperature field is evenly distributed and will slightly concentrate in the center. For the localized state, the temperature field tends to gather at the fourth ring, which is conformed with the eigenstate distribution. The temperature field also tends to concentrate at the ninth ring due to the localization of the second slowest branch. The eigenstate distribution of this state is shown in Fig. S1(c) of the Supplemental Material [42]. The decay rates of these two states are very close, so the thermal behavior of the second slowest branch is also very evident in the temperature field evolution. The double localization centers are unique in diffusion systems, which have no counterpart in the quantum systems and classical wave systems.

*Diffusive non-reciprocal AAH model.* To investigate the interplay between non-Hermitian skin effect and Anderson localization, we should introduce non-reciprocity into the AAH model. This model, which is the Hatano-Nelson model with incommensurate onsite energy, has three localized modes: skin mode localized at the right, Anderson localized mode, and skin mode localized at the left. Firstly, we should map the non-reciprocal AAH Hamiltonian onto the ring chain's Hamiltonian. Detailed derivation of diffusive non-reciprocal AAH Hamiltonian is shown in Part 2 of the Supplemental Material [42]. The eigenstate distributions of three localized modes are calculated in Fig. 2(a), (b), and (c). Here we label modes according to the behavior of the slowest branch. A winding number for non-reciprocity can be defined to characterize the behavior of bulk states as is shown in Part 2 of the Supplemental Material [42]. Next we should adjust the parameters to correspond to the non-reciprocal AAH model. The velocities of rings are set to zero. Except for the ring's thermal conductivity, the thermal conductivities of interlayers and the product of mass density and heat capacity of rings also need to be varied due to non-reciprocity and the expression of heat exchange rate. The parameters should be arranged as

$$\begin{aligned}\kappa_{I,j} &= a^{2(j-1)}\kappa_{I,1}, \quad j = 1, \dots, N-1 \\ \rho_j &= a^{2(j-1)}\rho_1, \quad j = 1, \dots, N\end{aligned}\tag{4}$$

Here we choose the mass density of rings to be varied and  $a$  is the non-reciprocal strength. For the three modes, the thermal conductivity of the first interlayer should be different to keep the adjusted thermal conductivities in a normal range. It can help to ensure the effect of skin effect is remarkable without extraordinarily long and short evolution time. The adjusted parameters for each ring and interlayer are shown in Fig. 2(d), (e), and (f). Detailed derivation of rings' adjusted thermal conductivities is shown in Part 2 of the Supplemental Material [42].

Then we study the temperature field evolution for three modes in the simulation, as can be seen in Fig. 2(g), (h), and (i). For right skin mode, the temperature field will gather to the most right ring. For Anderson localized mode, the temperature field tends to gather at the fourth ring, conformed with the result in Fig. 2(b). The temperature field also tends to accumulate at the first ring due to the localization of the second slowest branch, whose distribution is shown in Fig. S2(c) of the Supplemental Material [42]. For left skin mode, the temperature field will gather to the most left ring.

*Diffusive APT symmetric AAH model.* As another typical non-Hermiticity, we will introduce APT symmetry into the AAH model. One interesting thing is the extended-localized phase transition is in accordance with the APT transition point for the APT symmetric AAH model [13]. As usual, we should map the APT symmetric AAH Hamiltonian onto the ring chain's Hamiltonian. Detailed derivation of the Hamiltonian can be found in Part 3 of the Supplemental Material [42]. Since the bulk spectrum is insensitive to the boundary conditions, we set  $\alpha$  to be rational to imitate the periodic boundary condition [15]. A winding number for APT symmetry can be defined to characterize the topological properties of phase transition, as is shown in Part 3 of the Supplemental Material [42]. Here we choose an extended state (APT unbroken) and localized state (APT broken) for example. The eigenstate distributions of two states are calculated in Fig. 3(a) and (b). Next, the parameters should be adjusted to meet the diffusive APT symmetric AAH model. Here we choose the parameters  $\kappa_{l,j} = \kappa_l$ ,  $\rho_j = \rho$ , and  $C_j = C$  due to reciprocity. However, the onsite potential becomes complex for this model so the advection term should be introduced. The adjusted thermal conductivities and velocities of rings are shown in Fig. 3(c) and (d). Detailed derivation is shown in Part 3 of the Supplemental Material [42].

Next we perform the simulation of the temperature field evolution for two states, as is shown in Fig. 3(e) and (f). For the extended state, the temperature field is uniform. Besides, it is motionless because it is in the APT unbroken phase. However, there is no phase-locking effect [41] in this system. The reason is that it is quasiperiodic but not periodic and can not be considered as a

simple stack of double ring models. For the localized and APT broken state, the temperature field tends to gather at the tenth ring with a moving profile, conformed with the result in Fig. 3(b). The temperature field will also gather to the first ring because of the localization of the second slowest branch, which is shown in Fig. S3(d) of the Supplemental Material [42].

*Discussion and Conclusion.* We will propose a potential application of double localization centers, dubbed as non-Hermitian integrated double-trace distributed generator. In a thermal system, there often exist high temperature waste heat and low temperature waste heat. If the two positions of coupled ring chain structure are connected with high temperature waste heat and low temperature waste heat, also contacting with thermoelectric materials, external electricity can be generated. When the thermal system does not work, the high and low temperature heat sources will disappear. So the temperature field of the structure will evolve, and the double localization centers phenomenon will emerge. As seen in Fig. 4, we can choose the positions of thermoelectric materials as where the double localization centers appear. Then the generated power and duration of thermoelectric materials can be significantly enhanced compared with the structure without adjusting parameters, and two objects can be powered simultaneously. Besides, the locations of double localization centers can be set at will due to Anderson localization and APT (anti-parity-time) symmetry. Our device has a straightforward structure and flexible distributed power generation capabilities compared to the traditional electric generator.

Next, we also provide some experimental suggestions. Experimental setups in the Ref. [33] can be used to implement the diffusive AAH (Anbry-André-Harper) model, which is a coupled ring chain structure. However, the critical point is that the parameters of rings and interlayers should conform to the results of our theoretical calculation. So we recommend that some well-designed thermal metamaterials based on effective medium theory may meet our requirements here.

In summary, one-dimensional AAH model, a kind of quasicrystals, has been realized in diffusion systems through coupled ring chain structure for the first time. We can get the diffusive AAH Hamiltonian by carefully adjusting the parameters. Finite-element simulations confirm the existence of the extended state and localized state. For generalization, we introduce non-Hermitian skin effect and APT symmetry into the AAH model to investigate the interplay between Anderson localization and non-Hermitian physics. A novel double localization centers property can be found in the temperature field for Anderson localized state. We also propose a potential application named as non-Hermitian integrated double-trace distributed generator. We believe our results will motivate other researches on quasi-disordered and disordered phases in diffusion systems. For

example, the integer quantum Hall insulator in diffusion systems can be studied because it can map to the diffusive AAH model [43, 44]. Besides, these exotic phases of matter will help design novel thermal metamaterials for efficient and robust heat manipulation.

*Acknowledgments.* We thank Xinchun Zhou for helpful discussions. This work is supported by the National Natural Science Foundation of China under Grants No. 11725521 and No. 12035004 and the Science and Technology Commission of Shanghai Municipality under Grant No. 20JC1414700.

---

\* jphuang@fudan.edu.cn

- [1] S. Aubry and G. André, Ann. Isr. Phys. Soc. **3**, 133 (1980).
- [2] P. G. Harper, Proc. Phys. Soc. London Sect. A **68**, 874 (1955).
- [3] M. Kohmoto, Phys. Rev. Lett. **51**, 1198 (1983).
- [4] J. Biddle and S. Das Sarma, Phys. Rev. Lett. **104**, 070601 (2010).
- [5] G. Roati, C. D’Errico, L. Fallani, M. Fattori, C. Fort, M. Zaccanti, G. Modugno, M. Modugno, and M. Inguscio, Nature **453**, 895 (2008).
- [6] Q. Lin, T. Y. Li, L. Xiao, K. K. Wang, W. Yi, and P. Xue, arXiv:2112.15024 (2021).
- [7] Y. Lahini, R. Pugatch, F. Pozzi, M. Sorel, R. Morandotti, N. Davidson, and Y. Silberberg, Phys. Rev. Lett. **103**, 013901 (2009).
- [8] M. Verbin, O. Zilberberg, Y. E. Kraus, Y. Lahini, and Y. Silberberg, Phys. Rev. Lett. **110**, 076403 (2013).
- [9] C. H. Liang, D. D. Scott, and Y. N. Joglekar, Phys. Rev. A **89**, 030102 (2014).
- [10] C. Hang, Y. V. Kartashov, G. Huang, and V. V. Konotop, Opt. Lett. **40**, 2758 (2015).
- [11] A. K. Harter, T. E. Lee, and Y. N. Joglekar, Phys. Rev. A **93**, 062101 (2016).
- [12] Q. B. Zeng, S. Chen, and R. Lü, Phys. Rev. A **95**, 062118 (2017).
- [13] S. Longhi, Phys. Rev. Lett. **122**, 237601 (2019).
- [14] H. Jiang, L. J. Lang, C. Yang, S. L. Zhu, and S. Chen, Phys. Rev. B **100**, 054301 (2019).
- [15] S. Longhi, Phys. Rev. B **100**, 125157 (2019).
- [16] Q. B. Zeng, Y. B. Yang, and Y. Xu, Phys. Rev. B **101**, 020201 (2020).
- [17] Q. B. Zeng and Y. Xu, Phys. Rev. Res. **2**, 033052 (2020).
- [18] Z. H. Xu, X. Xia, and S. Chen, Sci. China-Phys. Mech. Astron. **65**, 227211 (2022).
- [19] A. P. Acharya, A. Chakrabarty, D. K. Sahu, and S. Datta, Phys. Rev. B **105**, 014202 (2022).
- [20] J. P. Huang, *Theoretical Thermotics: Transformation Thermotics and Extended Theories for Thermal Metamaterials* (Springer, Singapore, 2020).
- [21] S. Yang, J. Wang, G. L. Dai, F. B. Yang, and J. P. Huang, Phys. Rep. **908**, 1 (2021).
- [22] Y. Li, W. Li, T. C. Han, X. Zheng, J. X. Li, B. W. Li, S. H. Fan, and C.-W. Qiu, Nat. Rev. Mater. **6**, 488 (2021).
- [23] C. Z. Fan, Y. Gao, and J. P. Huang, Appl. Phys. Lett. **92**, 251907 (2008).



- [24] T. Y. Chen, C.-N. Weng, and J.-S. Chen, Appl. Phys. Lett. **93**, 114103 (2008).
- [25] W.-S. Yeung and R.-J. Yang, *Introduction to Thermal Cloaking: Theory and Analysis in Conduction and Convection* (Springer, Singapore, 2022).
- [26] Y. Li, X. Y. Shen, Z. H. Wu, J. Y. Huang, Y. X. Chen, Y. S. Ni, and J. P. Huang, Phys. Rev. Lett. **115**, 195503 (2015).
- [27] M. Camacho, B. Edwards, and N. Engheta, Nat. Commun. **11**, 3733 (2020).
- [28] L. J. Xu, G. Q. Xu, J. P. Huang, and C.-W. Qiu, Phys. Rev. Lett. **128**, 145901 (2022).
- [29] L. J. Xu, J. Wang, G. L. Dai, S. Yang, F. B. Yang, G. Wang, and J. P. Huang, Int. J. Heat Mass Transf. **165**, 120659 (2021).
- [30] G. Q. Xu, Y. Li, W. Li, S. H. Fan, and C.-W. Qiu, Phys. Rev. Lett. **127**, 105901 (2021).
- [31] G. Q. Xu, W. Li, X. Zhou, H. G. Li, Y. Li, S. H. Fan, S. Zhang, D. N. Christodoulides, and C.-W. Qiu, Proc. Natl. Acad. Sci. U. S. A. **119**, e2110018119 (2022).
- [32] L. J. Xu and J. P. Huang, EPL **134**, 60001 (2021).
- [33] G. Q. Xu, Y. H. Yang, X. Zhou, H. S. Chen, A. Alù, and C.-W. Qiu, Nat. Phys. **18**, 450 (2022).
- [34] T. Yoshida and Y. Hatsugai, Sci. Rep. **11**, 1 (2021).
- [35] S. Makino, T. Fukui, T. Yoshida, and Y. Hatsugai, Phys. Rev. E **105**, 024137 (2022).
- [36] M. H. Qi, D. Wang, P.-C. Cao, X.-F. Zhu, C.-W. Qiu, H. S. Chen, and Y. Li, Adv. Mater. , 2202241 (2022).
- [37] H. Hu, S. Han, Y. H. Yang, D. J. Liu, H. R. Xue, G.-G. Liu, Z. Y. Cheng, Q. J. Wang, S. Zhang, B. L. Zhang, and Y. Luo, Adv. Mater. , 2202257 (2022).
- [38] Z. F. Liu, L. J. Xu, and J. P. Huang, arXiv:2206.09837 (2022).
- [39] G. Q. Xu, X. Zhou, and C.-W. Qiu, arXiv:2206.11856 (2022).
- [40] P.-C. Cao, Y. Li, Y.-G. Peng, M. H. Qi, W.-X. Huang, P.-Q. Li, and X.-F. Zhu, Commun. Phys. **4**, 230 (2021).
- [41] P.-C. Cao, Y.-G. Peng, Y. Li, and X.-F. Zhu, Chinese Phys. Lett. **39**, 057801 (2022).
- [42] See Supplemental Material, which includes Ref. [13] and Ref. [14].
- [43] L. J. Lang, X. Cai, and S. Chen, Phys. Rev. Lett. **108**, 220401 (2012).
- [44] Y. E. Kraus, Y. Lahini, Z. Ringel, M. Verbin, and O. Zilberberg, Phys. Rev. Lett. **109**, 106402 (2012).

## FIGURE CAPTION

Fig. 1. Diffusive AAH model. (a) Schematic diagram of the coupled ring chain structure. The blue area indicates the ring, while the gray area represents the interlayer. The above is the three-dimensional diagram. For clarity, we transform rings into planar channels and set the periodic boundary condition at both ends, which is shown below. Here the down most channel is labeled as the first (most left) ring and the upmost channel is marked as the last (most right) ring. (b) The adjusted thermal conductivities for each ring. The eigenstate distribution of diffusive AAH Hamiltonian for the extended state (c) and localized state (d). The modes we consider here are the slowest decaying ones. Temperature field evolutions for the extended state (e) and localized state (f). Red and blue colors indicate the maximum and minimum temperatures. The initial condition is as following: The temperature  $T_h$  of the middle of channel is highest and  $T_l$  of the boundary of channel is lowest. The temperatures between these two positions are linearly distributed. The parameters are  $b = 12.5$  mm,  $d = 2$  mm,  $R = 100$  mm,  $\rho = 1000$  kg/m<sup>3</sup>,  $C = 1000$  J/(kg·K),  $\kappa_l = 1$  W/(m·K),  $M = 5$ ,  $\alpha = (\sqrt{5} - 1)/2$ ,  $T_h = 1093.2$  K and  $T_l = 293.2$  K. The number of rings is  $N = 10$ .

Fig. 2. Diffusive non-reciprocal AAH model. (a), (b) and (c) The eigenstate distribution of diffusive non-reciprocal AAH Hamiltonian for right skin mode ( $a = 0.14$ ), Anderson localized mode ( $a = 1.11$ ) and left skin mode ( $a = 7.39$ ). (d), (e) and (f) The adjusted thermal conductivities of rings, thermal conductivities of interlayers, and mass densities of rings. Here we adopt the logarithmic coordinates along  $y$ . For three modes, thermal conductivities of the most left (down most) interlayer are  $1 \times 10^5$  W/(m·K),  $0.1$  W/(m·K) and  $0.1$  W/(m·K) respectively. We define  $\kappa_D = 1$  W/(m·K) and  $\rho_D = 1$  kg/m<sup>3</sup> to eliminate the dimension. Temperature field evolutions for right skin mode (g), Anderson localized mode (h), and left skin mode (i). The initial condition is the same as in Fig. 1. The parameters are  $b = 12.5$  mm,  $d = 2$  mm,  $R = 100$  mm,  $\rho_l = 1000$  kg/m<sup>3</sup>,  $C = 1000$  J/(kg·K),  $M = 11$ ,  $\alpha = (\sqrt{5} - 1)/2$ ,  $T_h = 1093.2$  K and  $T_l = 293.2$  K. The number of rings is  $N = 8$ .

Fig. 3. Diffusive APT symmetric AAH model. (a) and (b) The eigenstate distribution of diffusive APT symmetric AAH Hamiltonian for extended state ( $\varphi = 0.5$ ) and localized state ( $\varphi = 2$ ). (c) and (d) The adjusted thermal conductivities and velocities for each ring. Temperature field evolutions for the extended state (e) and localized state (f). The initial condition is the same as in Fig. 1. The parameters are  $b = 12.5$  mm,  $d = 2$  mm,  $R = 100$  mm,  $\rho = 1000$  kg/m<sup>3</sup>,  $C = 1000$  J/(kg·K),

$\kappa_1 = 1 \text{ W/(m}\cdot\text{K)}$ ,  $M = 6$ ,  $\alpha = 6/11$ ,  $T_h = 1093.2 \text{ K}$  and  $T_l = 293.2 \text{ K}$ . The number of rings is  $N = 11$ .

Fig. 4. Non-Hermitian integrated double-trace distributed generator. The cuboid indicates the thermoelectric material. The temperature at the hot source, the temperature at the cold source, and the room temperature are denoted by  $T_H$ ,  $T_L$  and  $T_R$  respectively.

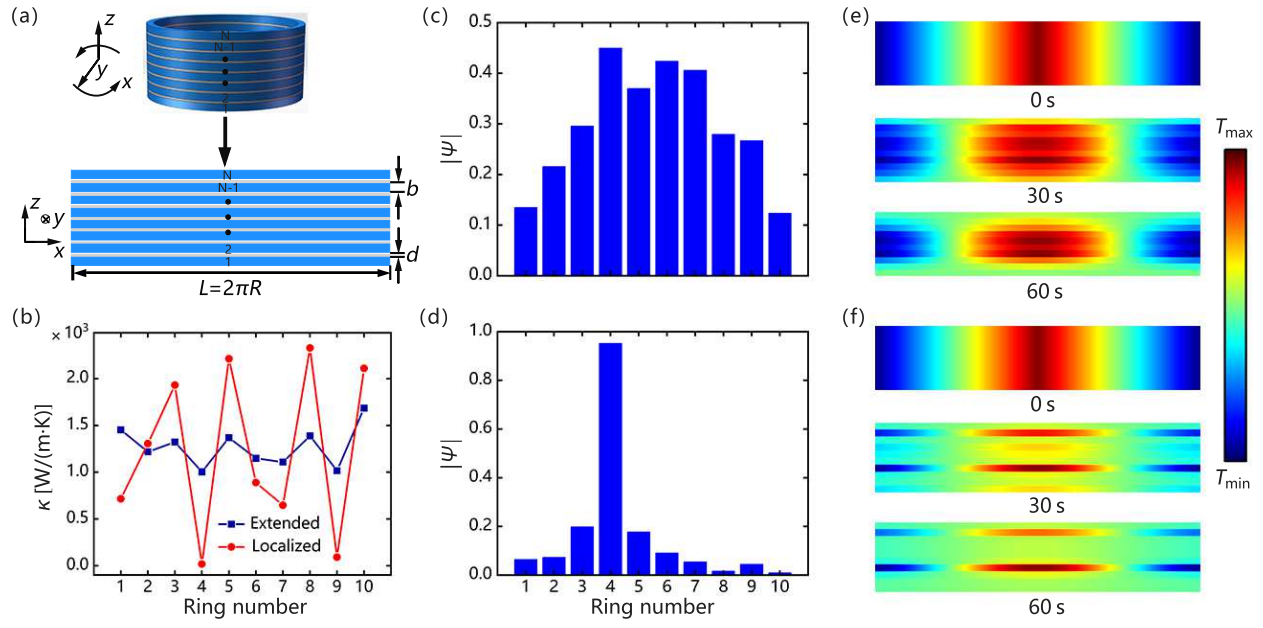


FIG. 1. Liu and Huang

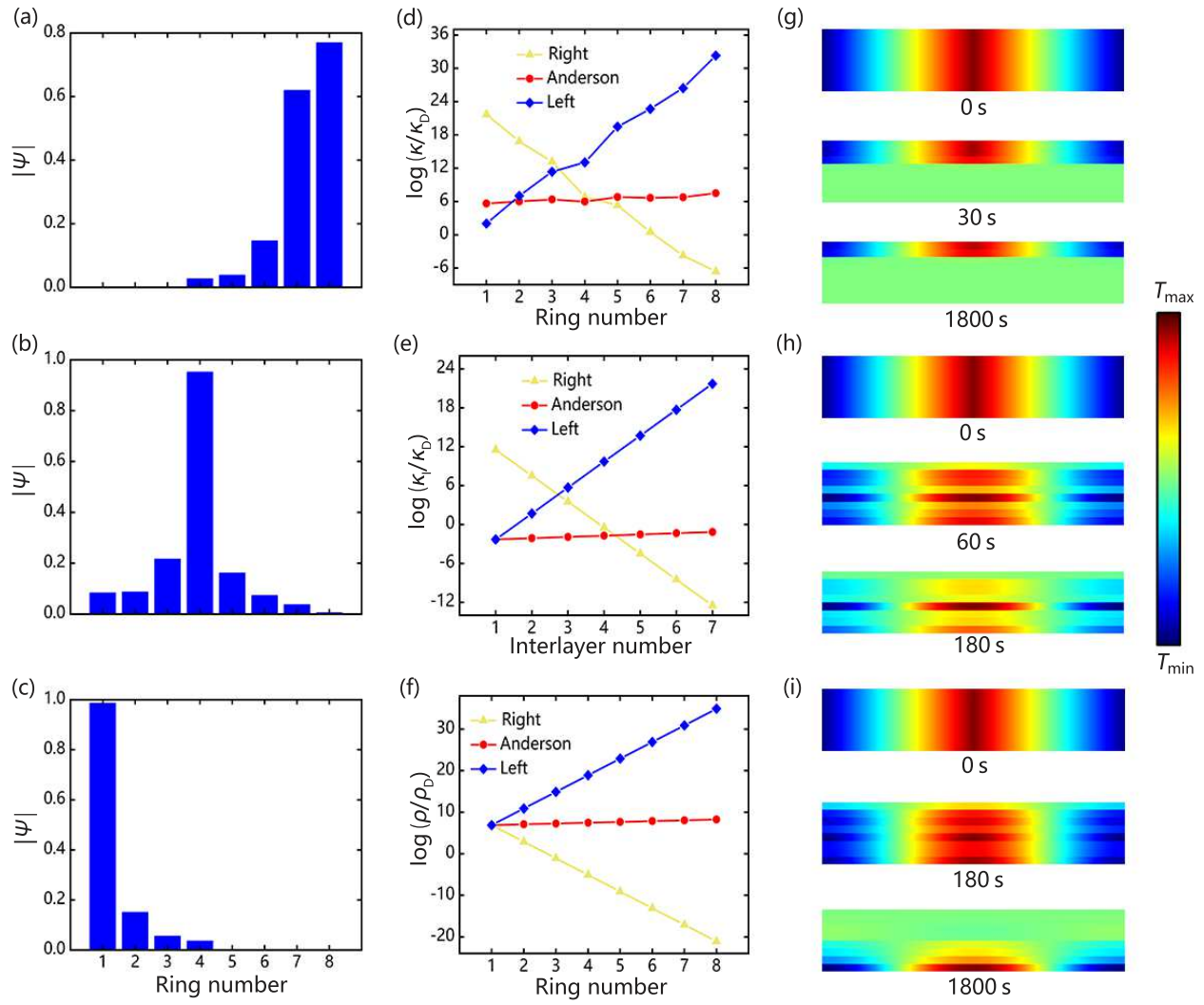


FIG. 2. Liu and Huang

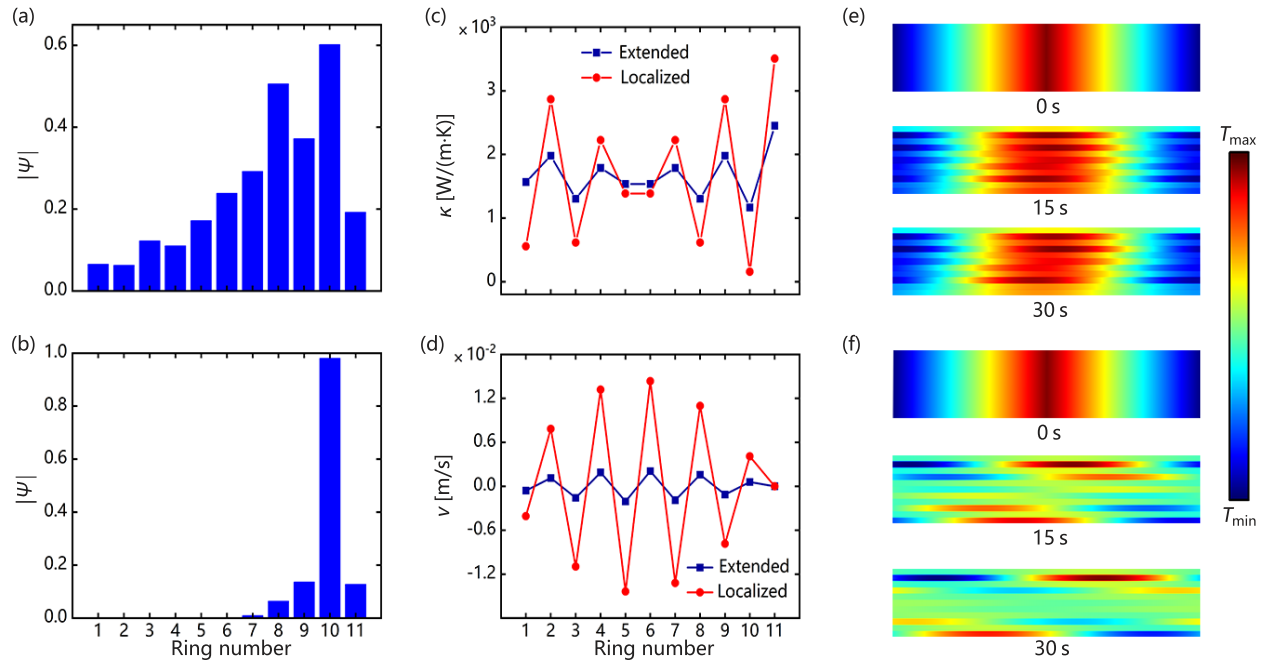


FIG. 3. Liu and Huang

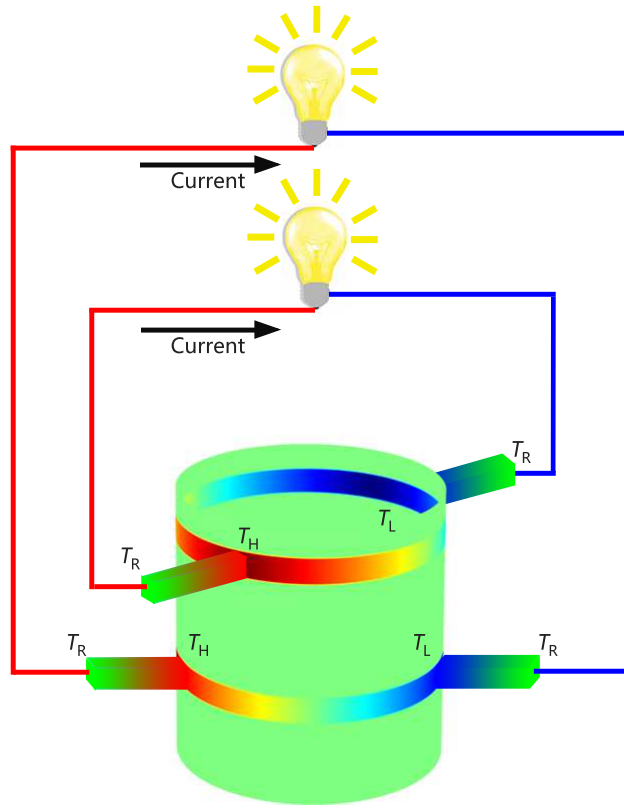


FIG. 4. Liu and Huang